

# Robust Stabilization of AVR Loop through Extended Reduced-Order Observer

Rittu Angu, R. K. Mehta

**Abstract:** An Extended Reduced Order Observer (EROO) based design approach has been presented for an Automatic Voltage Regulation (AVR) loop of the synchronous generator. The design approach utilizes the full state feedback to stabilize the AVR loop in the face of parameter uncertainty. The EROO-based design approach is capable of robust trajectory tracking in presence of parameter uncertainty and disturbances due to load demand changes. The design ensures specified stability margins at different speeds of response. An illustrative example has been provided to demonstrate the effectiveness of the methodology.

**Keywords:** Automatic voltage regulator, Control area, extended reduced-order state observer, augmented system, MATLAB simulation.

## I. INTRODUCTION

Power systems are large and complex electrical networks. The users of electrical power desire a reliable, uninterrupted and stable supply. However, it is not possible for a system to remain in steady state, since the load demands keeps on changing all the time [8] with rising or falling trend. The excitation system must contribute for the voltage control and enhancement of system stability. It must be able to respond quickly at any occurrence of disturbances enhancing the transient stability and the small signal stability. The function of the AVR is to provide constancy of the generator terminal voltage during normal, small and slow changes in the load. The regulation of system voltage magnitude automatically using AVR is also known as a Reactive Power control loop [1, 6] and influence the reactive power balances in the power system network. The AVR is achieved by the excitation mechanism. The excitation system can control the field current of the synchronous generator. Hence the field current is controlled so as to regulate the terminal voltage of a generator [5, 7]. The voltage of the generator is proportional to the speed and excitation of the generator. If we maintain a speed at constant level, then the excitation system can control the terminal voltage of the generator. The voltage control is also called as an excitation control system. For the generator, the excitation is provided by the main exciter. In present days, the exciter is a dc generator driven by either steam turbine or an induction motor. In modern vast interconnected power system manual control is not feasible, hence automatic equipments are installed on each generator.

**Manuscript Received on December 2014.**

Rittu Angu, M-Tech in Power System Engineering in 2013 from NERIST (Deemed University), Nirjuli Itanagar, India.

R. K. Mehta,

The objective of this work is to regulate the excitation of the system and deliver power in an interconnected system as stable as possible so that the voltages at various networks should not fall below or beyond permissible limits. The control strategy in this work attempts to utilize full state feedback for single area AVR controller design for a given plant conditions, the specifications set as [10]:

- (i) No deviation in magnitude of voltage in steady-state for a step change in load demand.
- (ii) Critical gain and phase margins must be greater or equal to the specified GM and PM.

It is assumed that the AVR model parameters (i.e.  $T_A$ ,  $T_E$ ,  $T'_{do}$ ,  $K_A$ ,  $K_E$  and  $K_F$ ) are given, output ( $\Delta|V|$ ) is available for feedback [1]. State feedback has potential to improve the performance of the AVR by judicious choice of closed-loop pole locations. An extended observer has been constructed to meet the performance requirements and iterative design steps are required to ensure satisfactory operation. The AVR model enhances disturbance rejection capability for the proposed control scheme. Moreover, a realistic AVR system having uncertain variations in parameters from their nominal values will be characterized by deviations in the nominal values of AVR parameters. In this paper, the parametric model uncertainty [4] has been considered, which represents imprecision of the parameters within the model. The extended observer-based closed-loop plant stability robustness studies have been carried out assigning a bound on the deviations in AVR system. Numerical results are presented to demonstrate the efficacy of the proposed control design procedure and to evaluate the performance and robustness qualities of the controller.

## II. PLANT MODEL

The AVR state model is based upon the open-loop transfer function model [1] as shown in Figure (1). Where  $G_A(s)$ ,  $G_E(s)$  and  $G_F(s)$  are amplifier, exciter and generator transfer functions. The state variables are chosen as

$$x = \begin{bmatrix} x_1 \\ x_2 \\ x_3 \end{bmatrix} = \begin{bmatrix} \Delta V_R \\ \Delta V_f \\ \Delta |V| \end{bmatrix}$$

The state model of open-loop AVR system with output as terminal voltage  $\Delta|V|$  is

$$\dot{x} = \begin{bmatrix} a_{11} & 0 & 0 \\ a_{21} & a_{22} & 0 \\ 0 & a_{32} & a_{33} \end{bmatrix} x + \begin{bmatrix} b_1 \\ 0 \\ 0 \end{bmatrix} u$$

$$y = [0 \ 0 \ 1] x$$

Where

$$\begin{aligned}
 a_{11} &= -\frac{1}{T_A} \\
 a_{21} &= \frac{K_E}{T_E} \\
 a_{22} &= -\frac{1}{T_E} \\
 a_{32} &= \frac{K_F}{T'_{do}} \\
 a_{33} &= -\frac{1}{T'_{do}} \\
 b_1 &= \frac{K_A}{T_A}
 \end{aligned}$$

The AVR model in the open loop has three real poles ( $-\frac{1}{T_A}, -\frac{1}{T_E}$  and  $-\frac{1}{T'_{do}}$ ) determined by the time constants of amplifier, exciter and generator transfer functions models. The system (A, B) is completely controllable. The proposed closed-loop control scheme for achieving desired transient and steady-state performance is discussed in the preceding section.

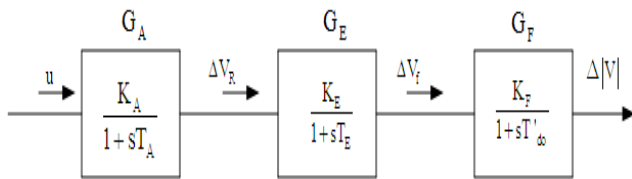


Figure 1: Block diagram of an open-loop AVR model

Figure 1 shows the block diagram of an uncontrolled single area power system. The state variable model for the system [2] is

$$\begin{aligned}
 \dot{x} &= Ax + Bu \\
 y &= Cx
 \end{aligned} \tag{1}$$

Where,

$$A = \begin{bmatrix} -\frac{1}{T_A} & 0 & 0 \\ \frac{K_E}{T_E} & -\frac{1}{T_E} & 0 \\ 0 & \frac{K_F}{T'_{do}} & -\frac{1}{T'_{do}} \end{bmatrix}, B = \begin{bmatrix} \frac{K_A}{T_A} \\ 0 \\ 0 \end{bmatrix} \text{ and } C = [0 \ 0 \ 1] \tag{2}$$

### III. EROO BASED CONTROL SCHEME

Figure 2 shows the full state feedback scheme based on an extended reduced-order observer (EROO). The open-loop AVR static model with terminal voltage ( $\Delta|V|$ ) as output is given by Equation (1). Where  $x = [x_1 \ x_2 \ x_3]^T$  and matrices A, B and C defined by Equation (2). The static variable  $x_3$  ( $\Delta|V|$ ) is measurable through a voltage sensor and it is assumed that  $x_1$  ( $\Delta|V_R|$ ) and  $x_2$  ( $\Delta|V_f|$ ) are to be estimated to eliminate the need for two sensors. So, the extended observer in Figure (2) is to be designed as third order system

to provide estimated variables  $\hat{x}_1, \hat{x}_2$  and  $\hat{d}$ . The state feedback gains ( $k_1, k_2$  and  $k_3$ ) are determined by pole-placement technique. The controller poles (closed-loop) have been decided considering the stability margin at X (Figure 2).

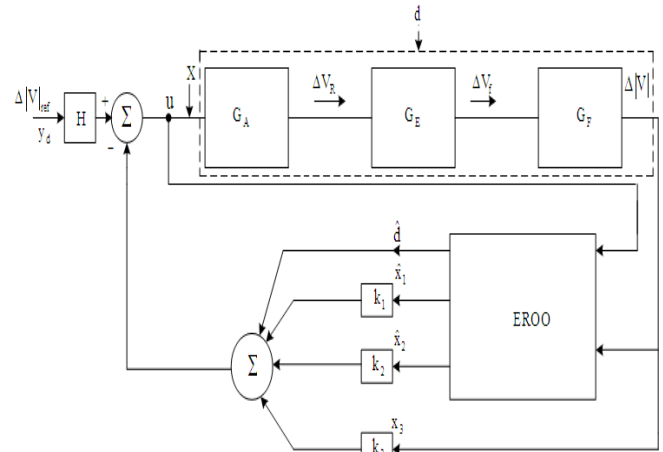


Figure 2: Closed-loop control scheme with EROO in feedback loop

### IV. EXTENDED REDUCED ORDER OBSERVER DESIGN

The extended reduced-order observer (EROO) design [9] has been carried out assuming a constant unknown disturbance appearing at the control output. Then, the disturbance dynamic can be given by  $\dot{d} = 0$ , resulting in  $A_d = 0$  and  $C_d = 1$ . Combining the plant with disturbance generator, the augmented plant in the state-space model is

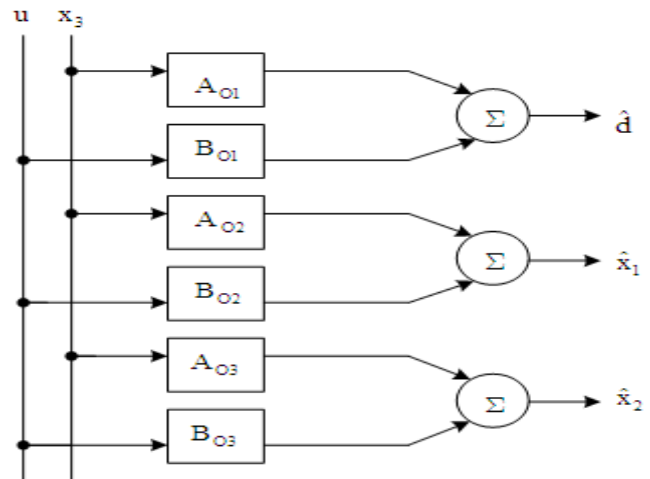


Figure 3: 3rd order extended observer

$$\begin{aligned}
 \dot{x}_a &= A_a x_a + B_a u \\
 y &= C_a x_a
 \end{aligned} \tag{3}$$

Where,  $x_a = [d \ x^T]^T$ . The matrices are

$$A_a = \begin{bmatrix} 0 & 0 & 0 & 0 \\ a_{11} & 0 & 0 & b_1 \\ a_{21} & a_{22} & 0 & 0 \\ 0 & a_{32} & a_{33} & 0 \end{bmatrix}, B_a = \begin{bmatrix} 0 \\ b_1 \\ 0 \\ 0 \end{bmatrix}, C_a = [0 \ 0 \ 1 \ 0]$$

If the pair  $(A_a, C_a)$  is observable and if system  $(A_a, B_a, C_a)$  does not have a zero, Equation (3) will be observable and an

observer (or reduced-order observer) can be constructed that will compute the estimates for  $x_1$  and  $x_2$  of plant and  $d$ . If form  $(-\hat{d})$  is added to the control (Figure 2), then it will cancel out the effects of the real disturbance. To construct third-order observer, the compatible transformation matrix on the basis of the augmented system (Equation 3) is introduced by

$$z = Tx_a = \begin{bmatrix} t_{11} & t_{12} & t_{13} & t_{14} \\ t_{21} & t_{22} & t_{23} & t_{24} \\ t_{31} & t_{32} & t_{33} & t_{34} \end{bmatrix} x_a \quad (4)$$

Where  $T$  is the  $3 \times 4$  matrix and  $z$  is the  $3 \times 1$  matrix. The third-order observer driven by  $x_3$  and  $u$ , but the control has additional form  $(-\hat{d})$ .

$$\dot{z} = Dz + Fx_a + Gu$$

$$u = -(k_1\hat{x}_1 + k_2\hat{x}_2 + k_3x_3) - \hat{d} + y_d$$

Where

$$z = [z_1 \ z_2 \ z_3]^T$$

$$D = \begin{bmatrix} 0 & 1 & 0 \\ 0 & 0 & 1 \\ -d_0 & -d_1 & -d_2 \end{bmatrix}$$

$$F = \begin{bmatrix} 0 & 0 & 0 & 1 \\ 0 & 0 & 0 & 0 \\ 0 & 0 & 0 & 0 \end{bmatrix}$$

$$G = \begin{bmatrix} g_1 \\ g_2 \\ g_3 \end{bmatrix}$$

The Luenberger's compatibility conditions to be satisfied [4] in the design of the observer are

$$TA - DT = F \quad (5)$$

$$G = TB_a \quad (6)$$

As a rule of thumb, the observer poles can be chosen to be faster than the controller poles by a factor of 2 to 6 [10], the third pole (real) of the observer due to disturbance dynamic has been placed such that the stability margins are satisfied. Thus, for known values for  $A$  and  $D$  matrices,  $T$ -matrix is obtained from Equation (5) using MATLAB program.

Using Equation (6),

$$G = TB_a = \begin{bmatrix} t_{12}b_1 \\ t_{22}b_1 \\ t_{32}b_1 \end{bmatrix}$$

The estimation of  $x_1$ ,  $x_2$  and  $d$  are denoted by  $\hat{x}_1$ ,  $\hat{x}_2$  and  $\hat{d}$  respectively can be obtained by rewriting the Equation (4) with partitioning between measured and observed state variables as

$$z = T_r x_r + T_m x_m \quad (7)$$

$$\text{Where } T_r = \begin{bmatrix} t_{11} & t_{12} & t_{13} \\ t_{21} & t_{22} & t_{23} \\ t_{31} & t_{32} & t_{33} \end{bmatrix}, T_m = \begin{bmatrix} t_{14} \\ t_{24} \\ t_{34} \end{bmatrix}$$

Here  $x_m = x_3$  is available for measurement and  $x_r = [d \ x_1 \ x_2]^T$  is to be estimated. The estimation of  $x_r$  can be recovered from Equation (7) according to:

$$x_r = Mz - Hx_m \quad (8)$$

$$M = T_r^{-1} = \begin{bmatrix} m_{11} & m_{12} & m_{13} \\ m_{21} & m_{22} & m_{23} \\ m_{31} & m_{32} & m_{33} \end{bmatrix} \quad (9)$$

$$H = T_r^{-1}T_m = \begin{bmatrix} h_{11} \\ h_{12} \\ h_{13} \end{bmatrix} \quad (10)$$

$$\text{And } \hat{x}_r = [\hat{d} \ \hat{x}_1 \ \hat{x}_2]^T$$

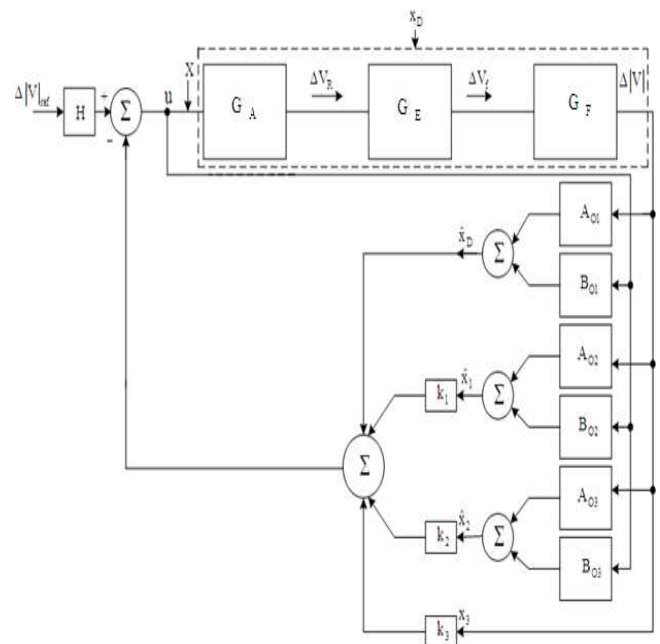


Figure 4: Closed-loop system with EROO in transfer function models

## V. CLOSED-LOOP POLE LOCATIONS

The main objective of optimal regulator or controller design known as linear quadratic regulator (LQR) is to define the performance index (cost function)  $J$  and search for  $u = -Kx$  that minimizes this index to stabilize the system (i.e. to transfer the system from its initial state to final state such that a given performance index is minimized). Consider the system

$$\dot{x} = Ax + Bu$$

The objective is to find the feedback  $K$  of control law such that the performance index

$$J = \int_0^{\infty} \rho y^2(t) + u^2(t) dt$$

is minimized for the system  $(A, B)$ . Here the optimal value of  $K$  is that which places the closed poles at the stable roots of the symmetric root locus equation [3]

$$1 + \rho G(-s)G(s) = 0 \quad (11)$$

In standard form

$$1 + \rho \frac{N(-s)N(s)}{D(-s)D(s)} = 0$$

Where  $G(s)$  is the open loop transfer function

$$G(s) = \frac{y(s)}{u(s)} = \frac{N(s)}{D(s)} = C(SI - A)^{-1} B$$

and  $\rho$  represent weighting penalties on the state variables and control inputs and is chosen by the designer. The controller's performance highly depends on the choice of the weighting factor  $\rho$ . Wrong choice of this may result to the frequency and power oscillating during disturbances. In reality, choosing different values of  $\rho$  can provide us with pole locations that achieve varying balances between a fast response and a low control effort. In practice, usually a value of  $\rho$  corresponding to a point close to the knee of the trade-off curve is chosen. This is because it provides a reasonable compromise between the use of control and the speed of response.

### Gain H

In order to achieve unity steady-state gain H (with EROO implemented in the loop) the overall transfer function  $|\Delta V|/|\Delta V_{ref}| = HG_{CL}(0)$  has been evaluated and then H was found as

$$H = \frac{d_0 K}{bo_{10} + d_0 + bo_{20}k_1 + bo_{30}k_2 + K(ao_{10} + ao_{20}k_1 + ao_{30}k_2 + d_0k_3)}$$

where,

$$K = K_A K_E K_F$$

$$ao_{10} = (-d_0 h_1 - d_0 m_{12} + d_1 m_{11}), \quad ao_{20} = (-d_0 h_2 - d_0 m_{22} + d_1 m_{21})$$

$$ao_{30} = (-d_0 h_3 - d_0 m_{32} + d_1 m_{31})$$

$$bo_{10} = (b_1 m_{11} t_{32} - b_1 d_0 m_{12} t_{12} + b_1 d_1 m_{11} t_{12} - b_1 d_0 m_{13} t_{22} + b_1 d_2 m_{11} t_{22})$$

$$bo_{20} = (b_1 m_{21} t_{32} - b_1 d_0 m_{22} t_{12} + b_1 d_1 m_{21} t_{12} - b_1 d_0 m_{23} t_{22} + b_1 d_2 m_{21} t_{22})$$

$$bo_{30} = (b_1 m_{31} t_{32} - b_1 d_0 m_{32} t_{12} + b_1 d_1 m_{31} t_{12} - b_1 d_0 m_{33} t_{22} + b_1 d_2 m_{31} t_{22})$$

### VI. STABILITY ANALYSIS

The open loop transfer function of the proposed system is obtained by opening its forward path and is solved by Mason's Gain formula for signal flow graph [2]. We consider the loop marked X in Figure 4 in our design approach to establish the stability margin in terms of open-loop gain responses. This is in-fact the ability of proposed system to deal successfully in-case of model uncertainties. The system is stable when gain values are increased but it may become unstable if the gain increases past a certain critical limit. The transfer function of open loop at X is

$$G_x(s) = \frac{N_1 s^3 + N_2 s^2 + N_3 s + N_4}{D_1 s^6 + D_2 s^5 + D_3 s^4 + D_4 s^3 + D_5 s^2 + D_6 s + D_7} \quad (12)$$

$$N_1 = K(ao_{13} + k_3 + ao_{23}k_1 + ao_{33}k_2)$$

$$N_2 = K(ao_{12} + ao_{22}k_1 + ao_{32}k_2 + d_2 k_3)$$

$$N_3 = K(ao_{11} + ao_{21}k_1 + ao_{31}k_2 + d_1 k_3)$$

$$N_4 = K(ao_{10} + ao_{20}k_1 + ao_{30}k_2 + d_0 k_3)$$

$$D_1 = R_2$$

$$D_2 = R_2 co_{12} + R_1$$

$$D_3 = R_2 co_{11} + R_1 co_{12} + R_0$$

$$D_4 = R_2 co_{10} + R_1 co_{11} + R_0 co_{12} + 1$$

$$D_5 = R_1 co_{10} + R_0 co_{11} + co_{12}$$

$$D_6 = R_0 co_{10} + co_{11}$$

$$D_7 = co_{10}$$

where,

$$ao_{13} = (-h_1), \quad ao_{23} = (-h_2), \quad ao_{33} = (-h_3)$$

$$ao_{12} = (m_{11} - d_2 h_1), \quad ao_{22} = (m_{21} - d_2 h_2), \quad ao_{32} = (m_{31} - d_2 h_3)$$

$$ao_{11} = (d_2 m_{11} - d_0 m_{13} - d_1 h_1)$$

$$ao_{21} = (d_2 m_{21} - d_0 m_{23} - d_1 h_2)$$

$$ao_{31} = (d_2 m_{31} - d_0 m_{33} - d_1 h_3)$$

$$bo_{12} = (b_1 m_{11} t_{12} + b_1 m_{12} t_{22} + b_1 m_{13} t_{32})$$

$$bo_{22} = (b_1 m_{21} t_{12} + b_1 m_{22} t_{22} + b_1 m_{23} t_{32})$$

$$bo_{32} = (b_1 m_{31} t_{12} + b_1 m_{32} t_{22} + b_1 m_{33} t_{32})$$

$$bo_{11} = (b_1 m_{11} t_{22} + b_1 m_{12} t_{32} - b_1 d_0 m_{13} t_{12} + b_1 d_2 m_{11} t_{12} - b_1 d_1 m_{13} t_{22} + b_1 d_2 m_{12} t_{22})$$

$$bo_{21} = (b_1 m_{21} t_{22} + b_1 m_{22} t_{32} - b_1 d_0 m_{23} t_{12} + b_1 d_2 m_{21} t_{12} - b_1 d_1 m_{23} t_{22} + b_1 d_2 m_{22} t_{22})$$

$$bo_{31} = (b_1 m_{31} t_{22} + b_1 m_{32} t_{32} - b_1 d_0 m_{33} t_{12} + b_1 d_2 m_{31} t_{12} - b_1 d_1 m_{33} t_{22} + b_1 d_2 m_{32} t_{22})$$

$$co_{12} = d_2 + bo_{12} + bo_{22}k_1 + bo_{32}k_2$$

$$co_{11} = d_1 + bo_{11} + bo_{21}k_1 + bo_{31}k_2$$

$$co_{10} = d_0 + bo_{10} + bo_{20}k_1 + bo_{30}k_2$$

$$R_2 = T_A T_E T'_{do}, \quad R_1 = T_A T_E + T_A T'_{do} + T_E T'_{do}, \quad R_0 = T_A + T_E + T'_{do}$$

Two commonly used quantities that measure the stability margin for such system are the gain margin (GM) and phase margin (PM). This is discussed in next section with respect to Bode plots of GM and PM.

### VII. SIMULATION AND RESULTS

With an objective to meet the specifications  $GM \geq 6$  dB,  $PM \geq 40$  degree and no voltage deviations in the steady-state, an extended reduced order state observer with full state feedback has been designed for the AVR model. A typical operating condition has been chosen as the nominal values of the parameters of the AVR model are shown in Table 1. A deviation of  $\pm 10\%$  on the nominal values of the parameters of AVR model has been considered for investigation of stability issues of the designed control scheme in Figure 4 for AVR model.

The closed-loop pole (CLP) locations have been chosen from the SRL plot for the equation (11) as shown in Figure 5. The closed-loop pole location is given by  $s = -\rho_i$ . With the help of three closed loop poles from SRL plot, feedback gain constants  $k_1$ ,  $k_2$  and  $k_3$  are obtained using augmented state model.

The third-order reduced observer has been designed with its pole locations are at 3.5 times the controller pole locations (obtained from SRL plot) to determine D-matrix. The matrices T, G and M have been determined using Equations (5), (6) and (9) respectively. The open-loop transfer function  $G_x(s)$  have been determined using equations (12) for stability margins analysis. Figure 6 indicates the variations in GM and PM at X with  $\rho$  for various values of  $\rho_i$ . It is observed that the GM and the PM remain almost constant with  $\rho$  in the higher range, but they vary appreciably with  $\rho_i$ . The critical PM occurs corresponds to loop opening at X.

In this paper,  $\rho=100$  and  $\rho_i=9$  have been selected to satisfy  $GM \geq 6$  dB and  $PM \geq 40$  degree. Table 2 shows the closed-loop pole locations and controller gains. The results of performance studies obtained by MATLAB simulations for the selected operating points are provided in Table 3 and 4. The results describing the disturbance rejection property for various load demand changes have been shown in Figure 7.

The unit step response for terminal voltage with step disturbance applied at  $t= 5$  sec. and under parameter uncertainties are shown in Figure 8 and 9 respectively.

**Table 1: Area parameter values**

Area Parameter	$T_A(\text{sec.})$	$T_E(\text{sec.})$	$T'_{do}(\text{sec.})$
Nominal value	0.1	0.4	1.0
Nominal value +10%	0.11	0.44	1.1
Nominal value -10%	0.09	0.36	0.9

**Table 2: Closed-loop pole locations and associated gains**

CLP for	CLP locations	Observer poles	Controller gains
$\rho=100$	$\lambda_2 = -12.17$	$d_2 = -94.16$	$k_1 = 0.24$
$\rho_i = 9$	$\lambda_1 = -5.56 + 7.16i$	$d_1 = -$ $2579.35$	$k_2 = 1.46$ $k_3 = 8.05$
	$\lambda_0 = -5.56 - 7.16i$	$d_0 = -$ $16316.40$	

**Table 3: Result of frequency response studies on proposed system**

Loop break at	Perturbation	GM (dB)	GCF (rad/sec)	PM (deg)	PCF (rad/sec)
X	Nominal	9.93	7.45	43.5	2.86
	+10%	9.94	6.76	43.7	2.59
	-10%	9.91	8.82	43.2	3.19

**Table 4: Settling time at varying load demands**

Load demand	Perturbation	Settling time (sec)	Maximum variation in frequency (Hz)
10%	Nominal	1.98	1.02
	+10%	2.18	1.02
	-10%	2.40	0.98
20%	Nominal	1.99	0.204
	+10%	2.18	0.204
	-10%	2.39	0.196

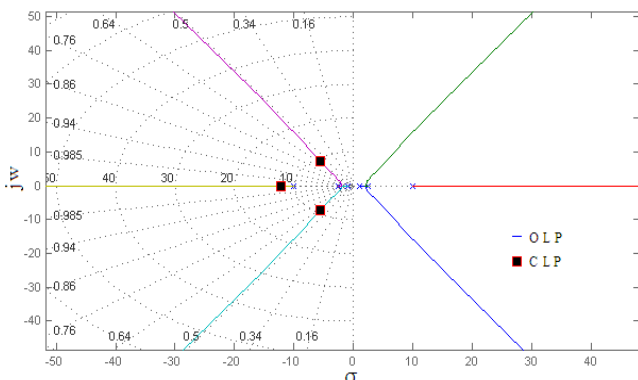


**Figure 5: Symmetrical root locus diagram with selected closed-loop poles**

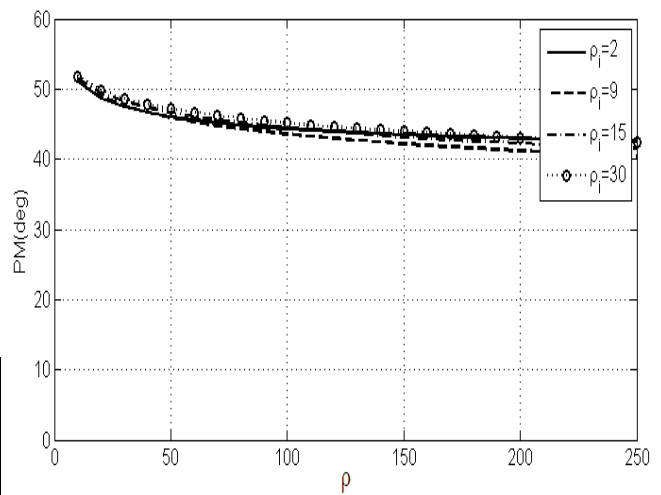
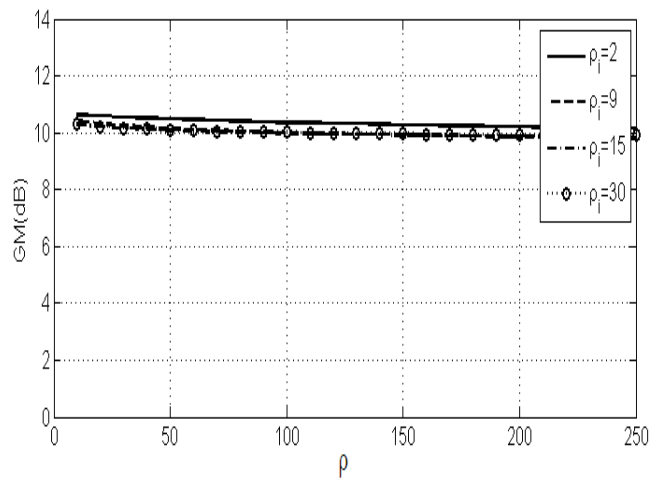


**Figure 6: GM and PM of the open-loop system (12) as a function of  $\rho$  for various values of  $\rho_i$**

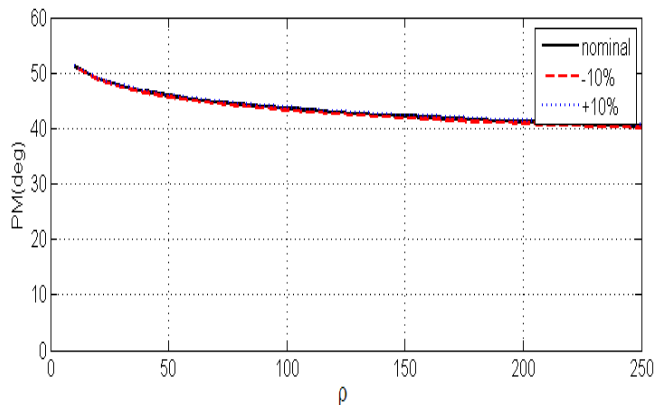
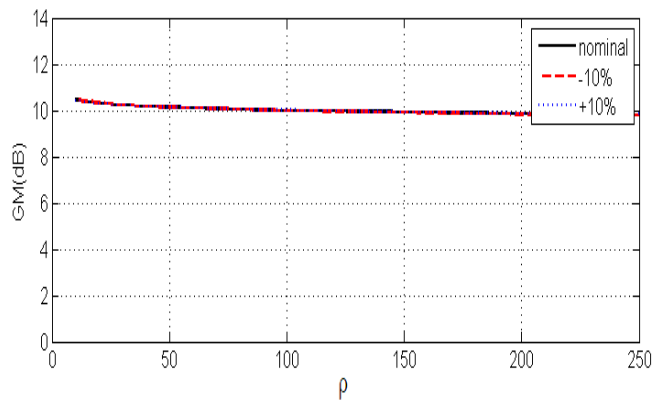


**Figure 7: GM and PM as a function of  $\rho$  under parameter variations**



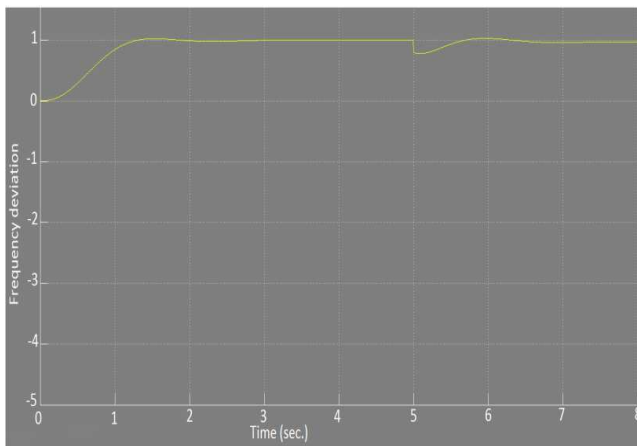


**Figure 8: Unit step response for terminal voltage with step disturbance applied at t= 5s**

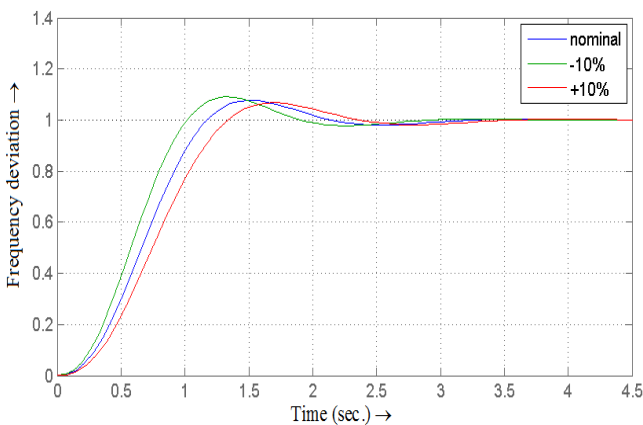


**Figure 9: Unit step response for terminal voltage under parameter uncertainties**

## VIII. CONCLUSION

In this paper, a reduced-order extended observer based control for AVR system has been presented. The designed system is very effective to compensate input disturbances as well as modeling uncertainties present in the AVR loop. It has been possible to estimate states (immeasurable) and the uncertainties as well as input disturbance in an integrated manner using EROO. It has also been observed that the EROO-based control improves tracking performance in presence of uncertainties and disturbances. The design enables to achieve desired specified stability margins in order to fully utilize the hardware resources by judiciously choosing the optimal speed of response in this design process.

## IX. NOTATIONS

$d_0, d_1, d_2$	coefficients of characteristic equation of extended reduced observer
$\lambda_0, \lambda_1, \lambda_2$	roots of characteristic equation of plant
$\rho$	system weighting penalty from SRL equation
$\pi$	weighting penalty assigned to system due to observer
$u$	control force/signal/input
$T_s$	settling time, sec.
$T_A$	amplifier time constant, sec.
$T_E$	exciter time constant, sec.
$T'd_0$	direct axis short circuit generator time constant, sec.

KA	gain of Amplifier, puHz/Mw
KE	gain of exciter, puHz/Mw
KF	gain of generator field, puHz/Mw
$k_1, k_2, k_3$	feedback gains
$e$	error signal
$s$	Laplace variable
$K(=KAKEKF)$	open loop gains

## REFERENCES

- [1] Olle I. Elgerd, Electric Energy Systems Theory; An Introduction (2nd Edition, McGraw-Hill Inc. 1982).
- [2] K. Ogata, Modern Control Engineering (4th edition, Prentice Hall Inc. 2002).
- [3] Gene F. Franklin, David Powell and Abbas Emami-Naeini, Feedback Control of Dynamic Systems (4th Edition, Pearsons Education Inc. 2002).
- [4] S.K. Goswami and K. Datta, On estimation errors in linear systems due to parametric variations, Journal of the institute of engineers (India), vol. 86, Dec. 2005, p(s) 192.
- [5] A. Soundarrajan, Member: Particle Swarm Optimization Based LFC and AVR of Autonomous Power Generating System, Proceeding on IAENG International Journal of Computer Science, 37:1, IJCS-37-1-10.
- [6] P. Kundur, Power System Stability and Control (McGraw-Hill Inc. 1994).
- [7] T. R. Shyama, Design of FGSPIC Controller Based Combined LFC and AVR of Two Area Interconnected Power Generating System, Proceeding on International Journal of Engineering and Advanced Technology (IJEAT) ISSN: 2249 – 8958, Volume-1, Issue-4, April 2012.
- [8] Prof. D.P. Kothari, Centre for Energy Studies on Automatic Generation Control, IIT Delhi, Lecture 24.
- [9] R.K. Mehta, S.K. Goswami and K. Datta, An observer -based lateral autopilot for tail-controlled missiles, IE(I) Journal-EL, Vol 88, sept. 2007, p(s): 17-22.
- [10] Dr. R.K. Mehta and Mr. Rittu Angu, An Observer-Based Robust Load Frequency Control, Journal of Electrical and Electronics Engineering, Vol. 9, Issue 4 Ver. I (Jul – Aug. 2014), P(s) 23-31.

## BIOGRAPHY

**Rittu Angu**, received his B.Tech. in Electrical Engineering in 2010 and M-Tech in Power System Engineering in 2013 from NERIST (Deemed University), Nirjuli Itanagar, India. At present, he is pursuing his Ph.D. degree in the same university. His area of interest includes power system quality control and electrical machines and drives